

Acrylic Acid-Grafted Hydrophilic Electrospun Nanofibrous Poly(L-lactic acid) Scaffold

Kwideok Park, Hyun Jung Jung, Jae-Jin Kim, Kwang-Duk Ahn, and Dong Keun Han*

Biomaterials Research Center, Korea Institute of Science and Technology, P. O. Box 131, Cheongryang, Seoul 130-650, Korea

Young Min Ju

Biomedical Engineering Program, University of South Florida, 4202 E. Fowler Avenue, ENB 118, Tampa, FL 33620, USA

Received July 18, 2006; Revised September 4, 2006

Abstract: Biodegradable nanofibrous poly(L-lactic acid) (PLLA) scaffold was prepared by an electrospinning process for use in tissue regeneration. The nanofiber scaffold was treated with oxygen plasma and then simultaneously in situ grafted with hydrophilic acrylic acid (AA) to obtain PLLA-g-PAA. The fiber diameter, pore size, and porosity of the electrospun nanofibrous PLLA scaffold were estimated as 250~750 nm, ~30 μm , and 95%, respectively. The ultimate tensile strength was 1.7 MPa and the percent elongation at break was 120%. Although the physical and mechanical properties of the PLLA-g-PAA scaffold were comparable to those of the PLLA control, a significantly lower contact angle and significantly higher ratio of oxygen to carbon were notable on the PLLA-g-PAA surface. After the fibroblasts were cultured for up to 6 days, cell adhesion and proliferation were much improved on the nanofibrous PLLA-g-PAA scaffold than on either PLLA film or unmodified nanofibrous PLLA scaffold. The present work demonstrated that the applications of plasma treatment and hydrophilic AA grafting were effective to modify the surface of electrospun nanofibrous polymer scaffolds and that the altered surface characteristics significantly improved cell adhesion and proliferation.

Keywords: tissue engineering, PLLA scaffold, electrospun nanofiber, plasma treatment, acrylic acid grafting, fibroblast.

Introduction

In tissue engineering, scaffold not only provides a three-dimensional (3D) structural architecture for target cells but also plays a dominant role in the control of cell adhesion, proliferation, and differentiation.¹ The main role of scaffolds is to directly transfer specific cells to a designated area or to grow them into a target tissue *in vitro*. An implanted scaffold is to be fully replaced with a regenerated tissue, along with a timely biodegradation of scaffold itself. Raw materials for scaffold fabrication are derived mostly from polymers, due to their easy processibility and flexibility to design into 3D structure. Scaffolds can take various forms, such as nonwoven mesh, sponge, and micro/nanospheres.²⁻⁴

Tissue engineering scaffolds need to be equipped with an architecture that is analogous to natural environment of target tissue in their composition, physical structure, and biological function. In this sense, nanofibrous polymer scaffolds have great advantages, due mainly to their dimensional and morphological homology to natural extracellular matrix (ECM)

components.⁵ For instance, since collagen is a network of nanometer-scale (50-500 nm) multi-fibrils, use of synthetic nanofibrillar matrix is supposed to closely realize the natural 3D environment of collagen matrix. In fact, scaffold architecture itself is of importance in associated with cell adhesion, proliferation, and differentiation on the surface. Compared to microscale scaffolds, because nanofibrous ones have larger surface areas to adsorb proteins, this structure can provide cells with much more binding sites available and consequently may help maintain phenotypic cell morphology.⁶ To produce nanofiber scaffold, electrospinning is a common method. In brief, once polymer is dissolved in an appropriate solvent, the polymer solution is fed in a syringe with needle. High voltage is applied to the solution to generate sufficient electric field to overcome the surface tension in a pendant drop of the polymer solution. As a polymer jet is drawn out of the needle orifice, these jets travel downward and become thinner as the solvent evaporates. This process produces nano-scale fibers in the path toward a collecting plate. These collected nanofibers are an entangled form of nonwoven mesh, and provide elasticity and tensile strength for nanofibrous structure. Upon the advancement of electrospinning technology,

*Corresponding Author. E-mail: dkh@kist.re.kr

nanofibrous polymer scaffolds are diverse in their polymer sources, fiber size, porosity, and texture. Biodegradable synthetic polymers, i.e., poly(L-lactic acid) (PLLA), poly(glycolic acid) (PGA), poly(lactic-co-glycolic acid) (PLGA), and poly(ϵ -caprolactone) (PCL) as well as natural polymers, such as collagen, silk proteins, and fibrinogen are fabricated into nanofibers via electrospinning.⁷ These nanofiber-based polymer scaffolds have been extensively applied for tissue-engineered cartilage, or bone, skin, and nerve.⁸⁻¹¹

While those biodegradable synthetic polymers are fairly biocompatible, their surfaces are hydrophobic and therefore cells are not preferentially attached to the surface. To improve the poor cell-adhesive characteristics, some advances have been achieved, transforming hydrophobic surface either physically or chemically into hydrophilic one. Some bioactive proteins, i.e., fibronectin, collagen, and laminin or Arg-Gly-Asp (RGD) peptide can be adsorbed on the polymer surface to increase cellular attachment.¹² Because the RGD sequence that is found in many ECM proteins provides a binding motif for cell adhesion, RGD peptide has been incorporated in hydrogels or polymer scaffolds in tissue engineering application.^{13,14} Chemicals were also useful to change surface characteristics. When PGA mesh scaffolds were treated with sodium hydroxide, the cell seeding density increased, due mainly to the chemically-modified surface with the hydrophilic functional groups.¹⁵ Pretreatment of electrospun PGA nanofibers in concentrated hydrochloric acid considerably improved cell attachment.¹⁶ As another modification methods, the use of electron beam, UV, and plasma has been documented.¹⁷⁻¹⁹ While the first two methods often compromise the mechanical property of scaffold, the impact of plasma treatment remains in an extremely limited depth and thus bulk properties of base materials are barely affected. During plasma discharge process, a functional group can be easily introduced on the substrate that has a complex 3D shape. Early studies showed that the plasma-treated substrates would have either direct or indirect effects on cellular response.²⁰⁻²³ Polymer surfaces on which hydrophilic monomers were grafted could directly elicit some notable effects with chondrocytes and human mesenchymal stem cells.^{20,21} On the other hand, grafted polymer surfaces were treated further with either RGD peptide or collagen to improve cell adhesion and proliferation.^{22,23}

The goal of this study is to investigate the efficacy of AA-grafted, hydrophilized nanofibrous PLLA scaffolds on fibroblast adhesion and proliferation in vitro for the direct applications to tissue engineering. The biodegradable nanofibrous PLLA scaffolds were made from electrospinning technique and then, both oxygen plasma treatment and in situ acrylic acid (AA) graft polymerization were simultaneously applied to nanofibrous hydrophobic PLLA scaffolds for surface modification. Bulk and surface properties of the surface-modified nanofibrous PLLA scaffolds as well as cell adhesion and proliferation on them were examined and compared to

unmodified ones.

Experimental

Materials. Biodegradable poly(L-lactic acid) (PLLA, MW: 110,000) was purchased from Boehringer Ingelheim (Germany). Acrylic acid (AA) as a hydrophilic graft monomer was bought from Aldrich (USA). All other chemicals were used in a reagent grade.

Preparation of PLLA Film. PLLA film was made using a solvent casting technique. When PLLA sample was dissolved in 8% chloroform, the polymer solution was uniformly mixed in the vortex mixing. This was then transferred to a glass plate and dried in vacuum for 48 hr to have PLLA film of 0.4-0.5 mm thickness.

Preparation of Nanofibrous PLLA Scaffolds. Nanofibrous PLLA scaffold was produced using electrospinning method as shown in Figure 1. The major components were ground electrode, high voltage power supply, 22-gauge needle, syringe, and collecting plate. Once PLLA was dissolved in the co-solvent (8/2, vol/vol), dichloromethane (DCM) and *N,N*-dimethylacetamide (DMAc), the polymer solution (8 wt%) was then fed in a syringe pump. The jet flow rate and high voltage power supply connected to the needle were set to 100~150 $\mu\text{L}/\text{min}$ and 15 kV, respectively. The distance between the needle tip and ground electrode was 10 cm. When an electric field was applied, ejection of the polymer jet began at the tip of the needle and the jet flow traveled downward. These nanoscale fibers were randomly deposited in the form of nonwoven mesh on the collecting plate to obtain nanofibrous PLLA scaffolds.

Preparation of Nanofibrous PLLA-g-PAA Scaffolds. Surface modification was carried out through oxygen plasma treatment and in situ graft polymerization of AA, a hydrophilic monomer using a radio frequency glow discharge (RFGD) device (Model PTS-003IDT, I.D.T. Eng., Inc., Korea). Briefly, nanofibrous PLLA scaffolds were put in the chamber of plasma-discharging device and fixed in between the electrodes that generate radio frequency. Once the valves were locked and internal chamber pressure reached to 10^{-3} torr,

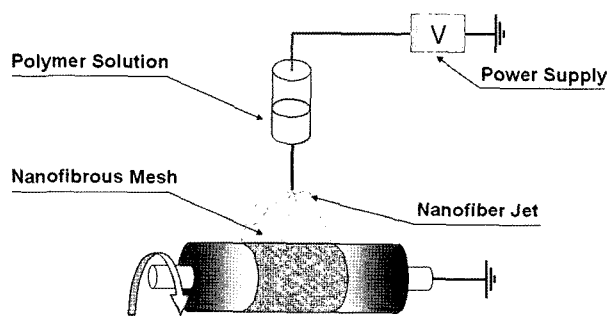


Figure 1. A schematic diagram of electrospinning process. Nanofibers are deposited in the form of nonwoven meshes.

oxygen in the gas phase was sprayed onto the scaffolds and subsequently AA was injected at the pressure of 0.2 torr. RF power (50 W) and pulse-type negative voltage were applied for the generation of plasma and maintained for 30 sec. After the operation was complete, the obtained nanofibrous PLLA-g-PAA scaffolds were washed with ethanol, dried in vacuum, and stored in a moisture-free condition for further use.

Bulk Characterization. For physical properties of nanofibrous PLLA-g-PAA scaffolds, each fiber diameter was directly read from the scale bar on scanning electron microscopy (SEM; S-2500C, Hitachi, Japan). Pore size was estimated from the distance between adjacent fibers in the non-woven mesh. Porosity was calculated from the previously reported equation.⁵ For mechanical properties, the scaffolds were tested for tensile strength and percent (%) elongation at break using an Instron testing machine (Model No. 4465, Instron, UK). Individual specimens were pulled uniaxially for tension break. Based on maximum load and initial surface area, ultimate tensile strength of each scaffold was determined. The % elongation was obtained from the ratio between initial (l_0) and elongated length (l) at the time of failure.

Surface Characterization. The post-treatment changes of surface properties were investigated for both PLLA film and nanofibrous scaffolds. Atomic composition at the surface was determined using an electron spectroscopy for chemical analysis (ESCA; S-Probe Surface Science, USA), which was equipped with AlK_{α} radiation source that can generate both voltage of 1,487 eV and power of 300 W at the anode. Water contact angles of PLLA film control and AA-grafted one were measured using a contact angle goniometer (VCA Optima XE Video Contact Angle System, Crest Technology, Singapore). They were averaged from five separate tests. Surface morphology of the nanofibrous scaffold was observed using SEM. Specimens were gold-coated using a sputter coater (Eiko IB3, Japan) for 5 min and each image was taken at 15 kV.

Fibroblast Culture. To evaluate the effect of surface

modification on cell adhesion and proliferation, NIH 3T3 fibroblasts were seeded at 1×10^5 cells/mL for PLLA film, nanofibrous PLLA scaffold, and nanofibrous PLLA-g-PAA scaffold (1×1 cm²), respectively. The culture medium was Dulbecco's Modified Eagles Medium (DMEM, Gibco, Grand Island, NY) supplemented with 10% fetal bovine serum (FBS; Gibco) and 1% penicillin/streptomycin (Gibco). During *in vitro* culture of the fibroblast/scaffold constructs in the humidified incubator at 37°C with 5% CO₂ supply, they were retrieved at specific time points (1, 3, and 6 days) and then subjected to SEM observation. The specimens were fixed with 2.5% glutaraldehyde for 16 hr at 4°C and dehydrated in a series of ethanol/water solution. For the extents to which cell proliferation proceeded on the different constructs, the 3-(4,5-dimethylthiazol-2-yl)-2,5-diphenyltetrazolium bromide (MTT) assay was used. Individual constructs were incubated with 1 mL MTT solution for 3 hr at 37°C in the 24-well plate. The samples were immersed in a lysis buffer (ethanol:DMSO=1:1) for 30 min. Once the lysates were then centrifuged at 200 g, the supernatant was collected and its absorbance was read using enzyme-linked immuno-sorbent assay (ELISA) system at 540 nm.

Statistical Analysis. The data were presented as means \pm standard deviation (SD). Statistically significant difference was determined using the Student *t* test. The difference was considered significant when *p* value is less than 0.05.

Results and Discussion

Bulk Properties of Nanofibrous PLLA Scaffolds. Once the electrospun nanofibrous PLLA scaffolds were made in electrospinning process, the fabricated nanofibers were found randomly deposited each other and the pore structure was formed in between nanofibers (Figure 2). The surface of PLLA film and nanofibers appeared to be smooth and especially, differences in the surface morphology were rarely visible in SEM observation between PLLA scaffolds and PLLA-g-PAA ones.

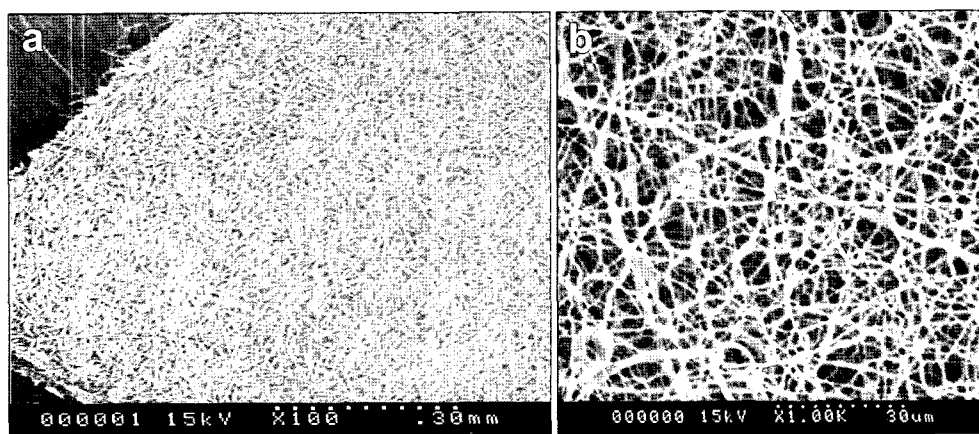


Figure 2. SEM images of electrospun nanofibrous PLLA-g-PAA scaffolds at low (a) and high (b) magnification.

The fiber diameter determined in SEM was ranged from 250 to 750 nm. Although different nanofiber diameter may be required, depending on tissue type, our results seemed to be reasonable compared to other reports. The average nanofiber diameter in poly(L-lactic-co- ϵ -caprolactone) copolymer scaffold was 550 ± 120 nm and that in collagen/elastin scaffold was ranged from 220 to 600 nm, changing with the different ratios between the two materials.^{24,25} In fact, electrospun nanofiber diameter can be controlled by adjusting flow rate of polymer solution, polymer concentration, solvent conductivity, and temperature. The primary benefit of these electrospun nanofibers is the similarity in fiber size to the natural ECM, because ECM itself is a delicately organized structure of nanofibers. These artificially reassembled nanofibrous PLLA scaffolds are thus expected to be effective for cell adhesion and proliferation.⁶ Pore size of the nanofibrous PLLA scaffolds ($\sim 30 \mu\text{m}$) was relatively smaller than that of the traditional nonwoven microfiber scaffolds that remained mostly in the range of hundreds of micron. Their porosity was 95% on average, which meant to be highly porous. The physical characteristics of nanofibrous polymer scaffolds are often variable, as materials and conditions are different. The porosity of nanofibrous PLGA scaffold was 92% and the pore size was broadly ranged from 2 to $465 \mu\text{m}$.²⁶ Polyurethane (PU) nanofiber scaffold carried 82.7% in porosity and 657 ± 183 nm in fiber diameter.²⁷ This significantly greater porosity would be advantageous, because higher porosity is believed to be preferable for cell seeding, adhesion and tissue growth in vitro, due to larger surface area-to-volume ratio. Such a property is also helpful for better diffusion of oxygen and nutrients into the inner area of scaffold.

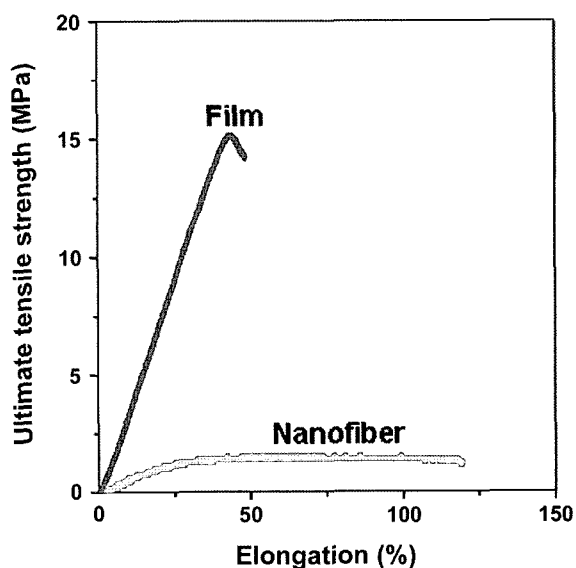


Figure 3. Mechanical properties of PLLA film and nanofibrous PLLA-g-PAA scaffolds. A typical load-displacement curve is presented.

On the other hand, as shown in the load-displacement curve (Figure 3), the ultimate tensile strength of nanofibrous PLLA scaffolds was 1.7 MPa on average, which was significantly lower than that of PLLA film, 15 MPa. The percent elongation at break was about 120 and 50% for nanofibrous scaffold and film, respectively. It is interesting to note that application of both plasma treatment and AA grafting made little difference on the bulk properties, including physical and mechanical ones, which was a definite advantage of the present modification method.

Surface Properties of Nanofibrous PLLA Scaffolds. Since the bulk properties of nanofibrous PLLA-g-PAA scaffolds were unable to reflect the subtle changes on the surface itself, surface analysis was of importance to identify differences from the original surface characteristics. When PLLA-g-PAA surface was analyzed (Table I), the result of ESCA showed that the percent (%) ratio of atomic composition of oxygen to carbon was substantially increased in the PLLA-g-PAA as compared to PLLA control. Water contact angles were also found significantly affected. The average contact angle of PLLA control surface was 75 degree, whereas that of PLLA-g-PAA surface was 45 degree. Both results strongly indicated that without altering the bulk properties, AA was successfully incorporated onto the PLLA surface, turning the original hydrophobic surface into hydrophilic one. It is notable that application of oxygen plasma treatment alone could also make surface hydrophilic but without AA grafting, the surface was very unstable, easily reoriented to the original surface property after 2 weeks. It was thus not suitable for our purpose. Impact of post-treatment should be significant on the surface chemistry and the following changes would mostly be compositional. Applied to 3D nanofiber structure, AA grafting should also be able to make the surface hydrophilic in the aid of plasma treatment. Presently used AA monomer that has a carboxylic group (-COOH) is easily applied in polymer surface grafting. The mechanism of plasma-induced modification is that once polymer chains are exposed to plasma glow discharge, radicals are generated and they react with monomers to produce hydrophilic functional groups on the surface, such as -OH, -NH₂, and -COOH.²⁸ It is very difficult to estimate graft yield of AA but from the previous quantitative assay, the concentration of the grafted AA on the PLLA film surface was 2×10^{-4} mmol/cm² (unpublished data).

While many polymer scaffolds are subjected to different

Table I. Surface Characteristics between PLLA Control and PLLA-g-PAA

Material	ESCA Atomic % (O _{1s} /C _{1s})	Contact Angle ^a (Degree)
PLLA control	0.61	75
PLLA-g-PAA	0.73	45

^aFilm.

modification protocols, few nanofibrous polymer scaffolds have been treated using the present method. Once electrospun PU microfibers were subjected to plasma-induced graft polymerization of negatively or positively charged monomers, they were implanted in rat subcutaneous dorsum to see the effects of various charges.²⁹ The *in vivo* data suggested that negatively charged surface might be better in vessel ingrowth into the microfibrinous mesh scaffold. In the study of Chua *et al.*, AA was grafted onto electrospun poly(carpolactone-co-ethylethylene phosphate) copolymer using UV irradiation.³⁰ After the surface was galactosylated further, rat hepatocyte spheroids were formed in smaller aggregates on the modified nanofiber scaffold, resulting in an integrated spheroid-nanofiber construct, which was not witnessed with microfiber scaffolds.

Adhesion Behavior of Fibroblast. Upon the preparation of electrospun nanofibrous PLLA scaffolds and following surface treatment and analytical works, it is thus of particular interest to see what effects of the altered surface would be on

cell behavior. We postulated that as compared to hydrophobic PLLA surface, hydrophilic PLLA-g-PAA one would have an added benefit for cell adhesion and proliferation. It is well-known that appropriately hydrophilic scaffold is more favorable for cell adhesion and proliferation.³¹ Once fibroblasts were seeded onto PLLA film, PLLA scaffold, and PLLA-g-PAA one, cellular responses on the different substrates were evaluated in terms of cell attachment and proliferation. After 24 hr post-seeding, compared to the film, more fibroblasts per unit area were found attached on the nanofibrous matrix, due to that surface areas for cell adhesion were significantly higher with the nanofibers (Figure 4). As the culture time was extended, highly proliferating cells were noticed on the hydrophilized PLLA-g-PAA scaffolds (Figure 5). During *in vitro* culture of fibroblasts on the three different polymer surfaces, the average cell number at 6 days reached to the highest level on the nanofibrous PLLA-g-PAA scaffolds (Figure 6). In addition, cell proliferation rate increased in the order of PLLA film, PLLA scaffold, and PLLA-g-PAA one.

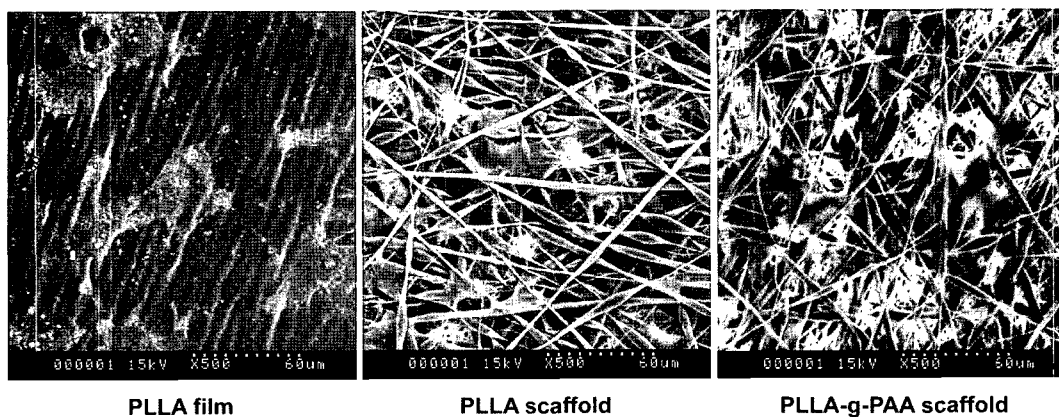


Figure 4. SEM micrographs of fibroblast adhesion after *in vitro* 24 hr culture on the PLLA film, nanofibrous PLLA scaffold, and PLLA-g-PAA scaffold, respectively.

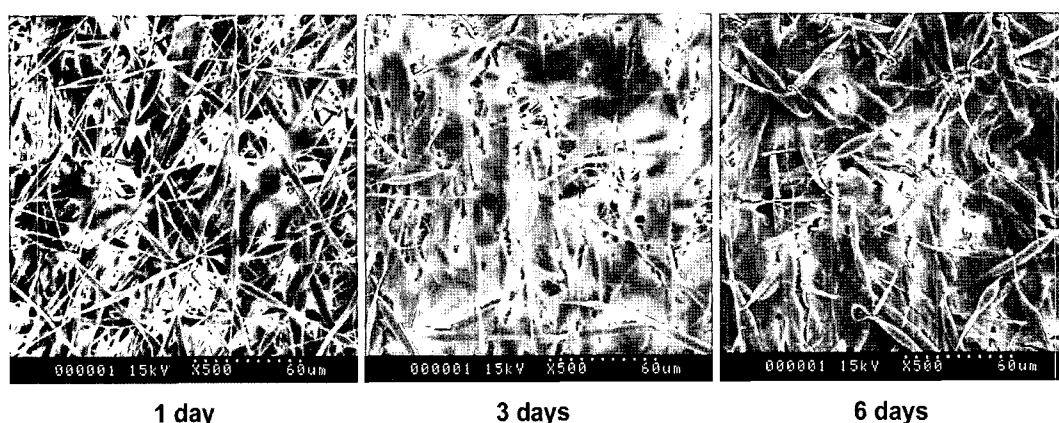


Figure 5. Fibroblast adhesion and proliferation on the nanofibrous PLLA-g-PAA scaffolds at different time points. As the culture time was extended, fibroblasts were being significantly proliferated.

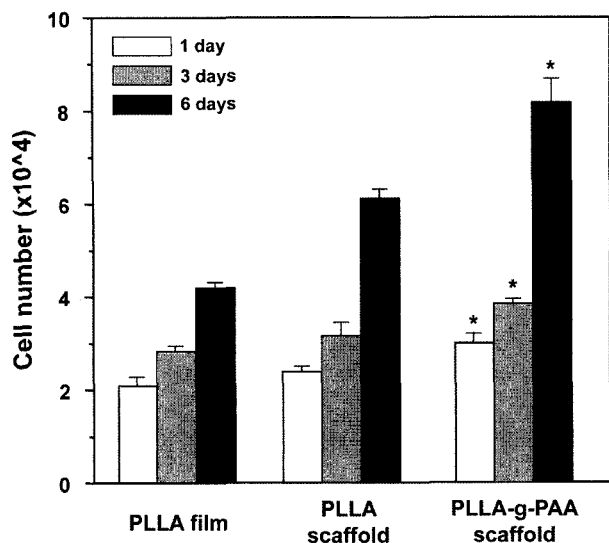


Figure 6. Proliferating activity of fibroblasts on the different PLLA substrates. As the cell numbers continuously increased with time, statistically significant differences (*: $p < 0.05$) were observed between nanofibrous PLLA-g-PAA scaffold and the others.

The fact that fibroblasts were more actively proliferating on the PLLA-g-PAA scaffold demonstrates the benefit of altered surface properties. The nanofibers could provide more cell-binding moieties for the cells through the hydrophilic AA grafting, as confirmed quantitatively in the surface analyses. Another benefit, not clearly identified in this study, may be that cellular infiltration can be improved with a hydrophilic surface and thus overall cellularity would increase in the scaffold. In addition to the effect of AA grafting, the role of serum proteins, i.e., fibronectin and vitronectin that contain cell-adhesive RGD sequence cannot be underestimated, because the grafted AA can serve as a linker between PLLA substrate and serum proteins to be immobilized onto it. It is thus plausible that the nanofibrous PLLA-g-PAA scaffold could immobilize even more serum proteins than the PLLA film or PLLA scaffold and these proteins should be advantageous, along with the pre-existed AA grafting, to significantly enhance fibroblast adhesion and proliferation on the PLLA-g-PAA surface. Previous study supports our results that scaffolds with nanofibrous pores were adsorbed with serum proteins four times more than the scaffolds with micropores and as a result, more osteoblastic cells were attached in the nanofibrous matrix.³² In another work, when poly(ethylene terephthalate) (PET) film surface was activated by plasma treatment, subsequently grafted with AA by thermal polymerization, and then coated with collagen type I, both PET-PAA and PET-PAA-collagen were tested with human smooth muscle cells.²³ The results showed that PET-PAA was better matrix for the cells than the films on which collagen was coated, because serum proteins could be spontaneously adsorbed on the AA-grafted surface, which

was very important step for cell adhesion and growth. Although the process of protein adsorption is hardly possible to be completely controlled, polymer scaffolds with well-defined surface characteristics would result in significant improvement of cell proliferation and differentiation during in vitro culture of tissue-engineered constructs.

Conclusions

After the electrospun nanofibrous PLLA scaffolds were made, their surface modification was successfully carried out with plasma treatment and subsequent in situ AA grafting. This process adopted a carboxylic group on the surface and thus made the surface hydrophilic without compromising the bulk properties. The PLLA-g-PAA surface exhibited significantly higher atomic percent of oxygen and lower contact angles, indicating the surface hydrophilized. The in vitro results of cell-scaffold interactions showed that fibroblast adhesion and proliferation were remarkably improved on the PLLA-g-PAA scaffold as compared to PLLA one. The present surface treatment should be useful as a mean of hydrophilization and the resultant nanofibrous PLLA-g-PAA scaffolds can be a suitable 3D support in the field of tissue engineering.

Acknowledgements. This work was supported by KIST grants, 2E19220 and 2E19362, from Ministry of Science and Technology, Korea.

References

- (1) R. Langer and J. Vacanti, *Science*, **260**, 920 (1993).
- (2) M. J. Honda, T. Yada, M. Ueda, and K. Kimata, *J. Oral Maxillofac. Surg.*, **62**, 1510 (2004).
- (3) G. Chen, T. Sato, T. Ushida, R. Hirochika, Y. Shirasaki, N. Ochiai, and T. Tateishi, *J. Biomed. Mater. Res.*, **67**, 1170 (2003).
- (4) S. W. Kang, O. Jeon, and B. S. Kim, *Tissue Eng.*, **11**, 438 (2005).
- (5) P. X. Ma and R. Zhang, *J. Biomed. Mater. Res.*, **46**, 60 (1999).
- (6) M. M. Stevens and J. H. George, *Science*, **310**, 1135 (2005).
- (7) Z. Ma, M. Kotaki, R. Inai, and S. Ramakrishna, *Tissue Eng.*, **11**, 101 (2005).
- (8) H. Yoshimoto, Y. M. Shin, H. Terai, and J. P. Vacanti, *Biomaterials*, **24**, 2077 (2003).
- (9) W. Li, R. Tuli, C. Okafor, A. Derfoul, K. G. Danielson, D. J. Hall, and R. S. Tuan, *Biomaterials*, **26**, 599 (2005).
- (10) K. S. Rho, L. Jeong, G. Lee, B. M. Seo, Y. J. Park, S. D. Hong, S. Roh, J. J. Cho, W. H. Park, and B. M. Min, *Biomaterials*, **27**, 1452 (2006).
- (11) F. Yang, R. Murugan, S. Ramakrishna, X. Wang, Y. X. Ma, and S. Wang, *Biomaterials*, **25**, 1891 (2004).
- (12) M. H. Ho, D. M. Wang, H. J. Hsieh, H. C. Liu, T. Y. Hsien, J. Y. Lai, and L. T. Hou, *Biomaterials*, **26**, 3197 (2005).
- (13) F. Yang, C. G. Williams, D. A. Wang, H. Lee, P. N. Manson, and J. Elisseeff, *Biomaterials*, **26**, 5991 (2005).

- (14) B. M. Min, G. Lee, S. H. Kim, Y. S. Nam, T. S. Lee, and W. H. Park, *Biomaterials*, **25**, 1289 (2004).
- (15) E. D. Boland, T. A. Telemeco, D. G. Simpson, G. E. Wnek, and G. L. Bowlin, *J. Biomed. Mater. Res.*, **71B**, 144 (2004).
- (16) J. Gao, L. Niklason, and R. Langer, *J. Biomed. Mater. Res.*, **42**, 417 (1998).
- (17) J. P. Nuutinen, C. Clerc, T. Virta, and P. Tormala, *J. Biomater. Sci. Polym. Ed.*, **13**, 1325 (2002).
- (18) Z. Ma, C. Gao, Y. Gong, and J. Shen, *Biomaterials*, **24**, 3725 (2003).
- (19) H. Chim, J. L. Ong, J.-T. Schantz, D. W. Huttmacher, and C. M. Agrawal, *J. Biomed. Mater. Res.*, **65A**, 327 (2003).
- (20) F. Mwale, H. T. Wang, V. Nelea, L. Luo, J. Antoniou, and M. R. Wertheimer, *Biomaterials*, **27**, 2258 (2006).
- (21) T. B. F. Woodfield, S. Miot, I. Martin, C. A. van Blitterswijk, and J. Riesle, *Biomaterials*, **27**, 1043 (2006).
- (22) M. H. Ho, L. T. Hou, C. Y. Tu, H. J. Hsieh, J. Y. Lai, W. J. Chen, and D. M. Wang, *Macromol. Biosci.*, **6**, 90 (2006).
- (23) I. Bisson, M. Kosinski, S. Ruault, B. Gupta, J. Hilborn, F. Wurm, and P. Frey, *Biomaterials*, **23**, 3149 (2002).
- (24) L. Buttafoco, N. G. Kolkman, P. Engbers-Buijtenhuijs, A. A. Poot, P. J. Dijkstra, I. Vermes, and J. Feijen, *Biomaterials*, **27**, 724 (2006).
- (25) C. Y. Xu, R. Inai, M. Kotaki, and S. Ramakrishna, *Biomaterials*, **25**, 877 (2004).
- (26) W. J. Li, C. T. Laurencin, E. J. Caterson, R. S. Tuan, and F. K. Ko, *J. Biomed. Mater. Res.*, **60**, 613 (2002).
- (27) C. H. Lee, H. J. Shin, I. H. Cho, Y.-M. Kang, I. A. Kim, K.-D. Park, and J.-W. Shin, *Biomaterials*, **26**, 1261 (2005).
- (28) B. Gupta, J. Hilborn, C. Hollenstein, C. Plummer, R. Houriet, and N. Xanthopoulos, *J. Appl. Polym. Sci.*, **78**, 1083 (2000).
- (29) J. E. Sanders, S. E. Lamont, A. Karchin, S. L. Golledge, and B. D. Ratner, *Biomaterials*, **26**, 813 (2005).
- (30) K.-N. Chua, W.-S. Lim, P. Zhang, H. Lu, J. Wen, S. Ramakrishna, K. W. Leong, and H.-Q. Mao, *Biomaterials*, **26**, 2537 (2005).
- (31) G. Khang, J. H. Choe, J. M. Rhee, and H. B. Lee, *J. Appl. Polym. Sci.*, **85**, 1253 (2002).
- (32) K. M. Woo, V. J. Chen, and P. X. Ma, *J. Biomed. Mater. Res.*, **67A**, 531 (2003).